Langmuir

Article

pubs.acs.org/Langmuir

From Stability to Permeability of Adhesive Emulsion Bilayers

Abdou R. Thiam,* Nicolas Bremond, and Jérôme Bibette

UPMC Universite Paris 06, CNRS UMR 7195, ESPCI ParisTech, 10 rue Vauquelin, 75231 Paris, France

ABSTRACT: Water drops dispersed in chloroform and stabilized with phospholipids become adhesive if a bad solvent for lipids, such as silicone oil, is added to the continuous phase. In this way, two sticking drops are separated by a bilayer of phospholipids. By using microfluidic technologies, we probe the stability and properties of such membranes likewise encountered in foams or vesicles. We first establish the stability diagram of adhering drop pairs as a function of the continuous phase composition. We found two regimes of destabilization of the bilayer. The first one concerns a competition between the dynamics of adhesion and the transport of surfactants toward the interfaces that leads to a dilute surfactant coverage. The second one corresponds to a dense surface coverage where the lifetime distribution of the bilayer exponentially decreases as a signature of a nucleation process. In the stable regime, we observe the propagation of adhesion among a concentrated collection of drops. This is another remarkable illustration of the suction consequence when two close deformable objects are pulled apart. Moreover, the present experimental strategy offers a novel way to study the phase diagrams of bilayers from a single phospholipid to a mixture of phospholipids. Indeed, we detect phase transitions at a liquid−liquid interface that are ruled by the amount of bad solvent. Finally, we probe the transport of water molecules through the bilayer and show that its permeability is linked to the adhesion energy that reflects its fluidity.

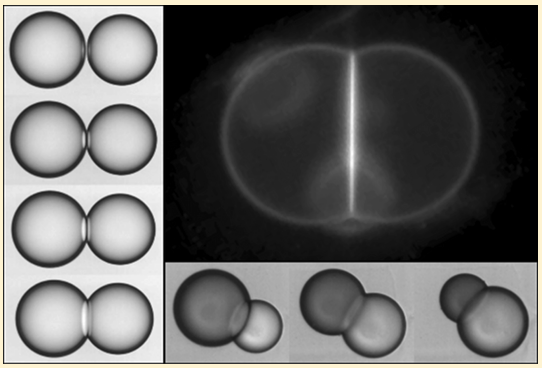

INTRODUCTION

The interaction between close interfaces is a widespread phenomenon[1,2] whose understanding is, for example, crucial for controlling the stability of colloidal solutions or thin liquid films. For emulsions or foams, a common way to stabilize such systems is to add surface active agents that delay the coalescence of neighboring drops or bubbles. Inverse emulsions are known to easily become adhesive[3] and therefore lead to the formation of a surfactant bilayer between drops. The stability and properties of such bilayers are of great interest because model membrane bilayers have been intensively prospected since many years now, most of the time for the sake of reconstituting biological membranes that are composed by a matrix of phospholipids.[4] Using inverse emulsion droplets to form such bilayers has already been achieved.[5,6] For mimicking purpose, the main parameter to control is the fluidity state of the bilayer that monitors many of the membrane properties[7,8] such as its permeability to molecules. For example, water molecules, which exhibit a high permeability to liposome membranes in the fluid phase state, are much less permeable to them in the gel phase. Likewise, ions or big polar molecules are weakly permeable to them[9,10] in both cases. One of the advantages to working with adhesive emulsions is the possibility of modifying the bilayer fluidity by tuning the adhesion energy via the continuous phase composition.[11]

In this paper, the stability and properties of phospholipid bilayers are probed by combining the use of adhesive emulsions and microfluidic technologies. When water drops are dispersed in an organic solvent and stabilized with surfactants, they become adhesive once a bad solvent for the surfactants is added to the continuous phase. Such adhesive inverse emulsions have been achieved by using a mixture of ether, a good solvent of the phospholipids, and silicone oil, the bad solvent.[5] This formulation favors the formation of surfactant bilayers at the expense of monolayers. There are other ways to form adhesive emulsion,[6,12,13] but the former one is a versatile and easy formulation. Moreover, the generated membrane has the targeted bilayer configuration leading to an interaction of the hydrophobic tails. As a matter of fact, bulk experiments usually lead to average measures, and the interaction between two objects is difficult to monitor. A dual micropipet setup can be employed to probe the interaction between two emulsion drops that may adhere or not.[14,15] As previously demonstrated, the use of microfluidic technology offers efficient means to quantitatively probe the stability of an emulsion at the level of a drop pair[16,17] or a collection of drops.[18,19] This experimental approach allows one to produce calibrated emulsion drops[20] and more importantly to uncouple the formation and the destruction steps of the emulsion. Here, we follow the same strategy in order to create isolated adhesive drop pairs[11] and then to characterize the bilayer properties.

Along that way, we first investigate the stability of the emulsion as a function of the phospholipid concentration and the mass fraction of bad solvent. Two regimes of destabilization of the bilayer are found. These regimes are linked to the surfactant coverage that is either dilute or dense. For high

Received: January 22, 2012
Revised: March 15, 2012
Published: March 22, 2012

concentrations of bad solvent, the phospholipids become insoluble in the oil mixture, and the emulsion spontaneously destabilizes precluding any adhesion. Then, we study the phase diagrams of bilayers that are composed of a single phospholipid and a mixture of phospholipids. We observe phase transitions at a liquid−liquid interface that are ruled by the amount of bad solvent. Finally, we probe the transport of water molecules through the bilayer as a function of the adhesion energy that reflects its fluidity.

MATERIALS AND METHODS

Adhesive inverse emulsions are formed following the footsteps of the work of Poulin et al.[5] Here, the organic phase is composed by a mixture of silicone oil, having a viscosity of 50 mPa.s and a density of 0.965, and chloroform for dispersing the phospholipids. We use three kind of phospholipids (Avanti Polar Lipids): 1,2-dihexadecanoyl-*sn*-glycero-3-phosphocholine (DPPC), 1,2-dipalmitoleoyl-*sn*-glycero-3-phosphocholine ((Δ9-Cis)PC) and 1-palmitoyl-2-(12-[(7-nitro-2-1,3-benzoxadiazol-4-yl)amino]dodecanoyl)-*sn*-glycero-3-phosphocholine (NBD-PC). Contrary to the previous formulation,[5] chloroform is preferred to diethyl ether to play the role of the good solvent because it is less volatile and swells less poly(dimethylsiloxane) (PDMS) microfluidic devices. Chloroform also has a high vapor pressure, and therefore working in hermetic circuits is a necessary condition to control the continuous phase composition. Moreover, even though the continuous phase contains enough surfactants to ensure a fast and full covering of the water droplets, above the critical micellar concentration, the adhesive emulsion is still highly unstable and breaks down within a few seconds. The presence of 150 mM of $MgSO_4$ (or down to 4 mM) in water droplets tremendously increases their lifetime[5,21] to more than a day.

Emulsion droplets are first formed in glass capillaries using the flow focusing technique[22] as presented in Figure 1a. Two round glass capillaries of 1 mm outer diameter are stretched and then cut with a microforge. The left capillary in Figure 1a is used for the aqueous phase injection and has a 80 μm aperture diameter, the right one sets for the main flowing channel and is 200 μm in diameter. The two round capillaries are embedded in a square glass capillary of 1 mm internal edge and separated by a distance of 100 μm (all capillaries are purchased from Vitrocom). The organic phase flows through the corners of the square capillary. To prevent any leakage, a high solvent resistant glue (Loctite glue, Manutan) is used for assembling the glass capillaries and tubes for liquid injection. In addition, to prevent any the wetting of water on glass walls, the capillaries are silanized with an octachloro(trimethyl)silane (Sigma) after a plasma cleaning. Thus, as soon as the different flows meet at the mouthpiece, water drops are regularly formed as shown in Figure 1a. Furthermore, we use PDMS devices because it is a low cost way to easily design drop traps used for observations of long duration. Moreover, since chloroform can evaporate through the PDMS matrix, the oil composition can be modified on-chip. We finally note that all experiments are performed at room temperature.

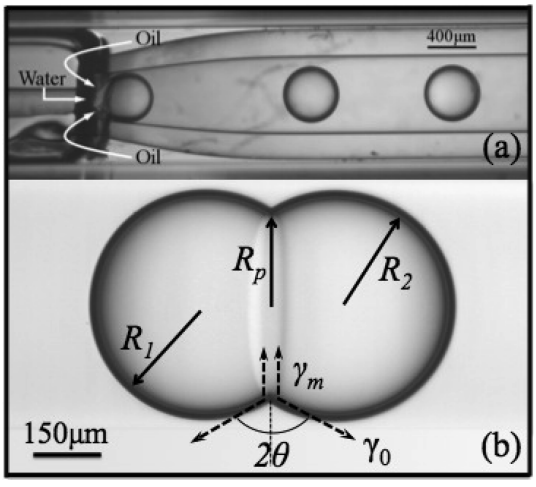

Figure 1. (a) Formation of water-in-oil emulsion drops by using a flow focusing configuration in a glass capillary device. (b) Snapshot of two adhesive drops along with the main parameters of the drop pair: R_1 and R_2 are the adhesive drops' radii, R_p is the radius of the patch, θ is the contact angle, γ_0 is the bulk interfacial tension of water/oil mixture in the presence of phospholipids, and γ_m is the surface tension of a monolayer composing the bilayer.

RESULTS AND DISCUSSION

Formation and Stability of Adhesive Drops. As shown in Figure 1a, a regular train of water in oil droplets is formed by a flow focusing method in glass capillaries. In order to induce the collision of two neighboring drops, the flow rate of the continuous phase is modulated. Indeed, this modulation leads to a slight variation of drop size which have therefore different velocities and eventually come into contact. Two drops that collide may ultimately adhere, as shown in Figure 1b. The adhering drops are thus separated by a phospholipid bilayer. The adhesion energy ΔF of the drop pair can be derived from the Young-Dupre equation:

$$\Delta F = 2\gamma_0(1 - \cos(\theta)) \quad (1)$$

where the contact angle θ is given by $2\theta = \sin^{-1}(R_p/R_1) + \sin^{-1}(R_p/R_2)$, R_p and $R_{1,2}$ denote for patch and drops radii (Figure 1b), and γ_0 is the surface tension of water and chloroform/silicone oil interface saturated with phospholipids. This surface tension γ_0 is measured by the micropipet aspiration technique[23] and found to be around 1 mN/m for an oil mixture having a mass fraction of bad solvent φ equal to 0.1 and with an excess of phospholipids. This value does not significantly vary when more bad solvent is added as long as phospholipids remain soluble in the oil mixture. We reasonably consider this value constant for other oil mixtures since the water/chloroform and water/silicone oil interfacial tensions are not too different in the absence of phospholipids (27 and 22 mN/m, respectively). Therefore, the adhesion energy ΔF essentially depends on the contact angle between drops, a parameter that is easily measurable. Then, by changing the oil composition and the phospholipids concentration, the evolution of the adhesion energy can be determined to characterize the system.

Let us first observe the formation of an adhesive drop pair. We note two main behaviors that depend on the organic phase composition: either the drops coalesce (Figure 2a) or the pair lasts hours (Figure 2b). The time needed for the adhesion patch to reach its maximal size is of the order of 1 s. As it will be discussed later, the drops can coalesce while the patch is growing or after having reached its equilibrium size. What happens if we consider a collection of drops? As reported in Figure 2c, once an adhesion is initiated between two drops among a compact train of drops, the adhesion starts to

dx.doi.org/10.1021/la3003349 | *Langmuir* 2012, 28, 6291−6298

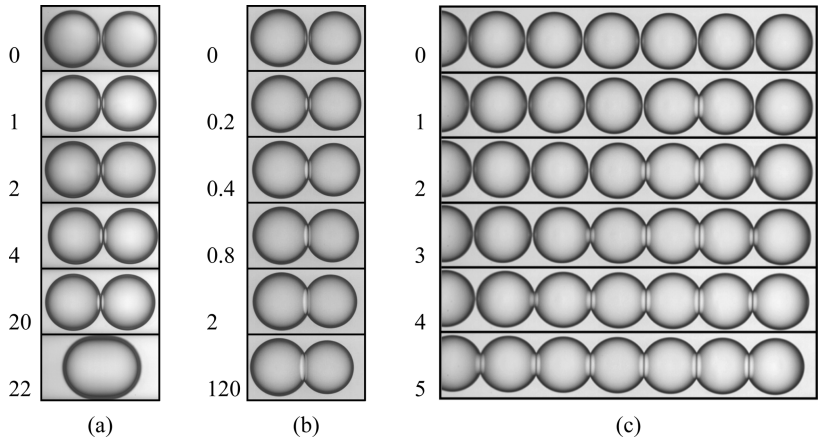

Figure 2. (a) Formation and destabilization of an adhering drop pair where $\varphi = 0.15$ and $C_{DPPC} = 10^{-3}$ wt %. (b) Formation of a stable adhesive pair where $\varphi = 0.25$ and $C_{DPPC} = 5 \times 10^{-3}$ wt %. (c) Propagation of the adhesion in a compact train of drops. The diameter of the drops is 220 μm, and the time for each image sequence is indicated in seconds.

propagate along the whole train. This cascade of adhesion reminds us of the propagation of coalescence arising in a concentrated emulsion.[16,19] We have demonstrated that the separation of two neighboring emulsion drops favors their coalescence. Indeed, the separation leads to a pressure reduction in the interstitial film between the two drops that induces a bulging out of the interfaces.[24−26] Therefore, the two interfaces get locally closer, allowing coalescence or adhesion to be nucleated. For a concentrated emulsion, the shape relaxation between the first drops that coalesce or adhere spontaneously results in a separation with their neighboring drops, a situation that potentially triggers further coalescence or adhesion. The cascade of adhesion reported in Figure 2c is thus another remarkable illustration of the suction phenomenon, and its consequences, arising when two deformable neighboring objects are pulled apart.

As observed in Figure 2, the bilayer lifetime depends on the phospholipids concentration and the organic phase mixture. We now focus on the stability of adhesive emulsion bilayers as a function of the formulation. In practice, for each condition, adhesive drops are formed in glass capillaries and, their stability against coalescence is followed over 5 min. If a drop pair last longer, then the bilayer is considered as stable, and very often it stays stable over a full day. The stability diagram for DPPC is reported in Figure 3. First, the stability of the bilayers requires an increase of the phospholipid concentration concomitant with the amount of bad solvent φ. Second, when the emulsion is directly formed beyond a critical bad solvent composition, $\varphi^* = 0.58$, it immediately coalesces, whatever the DPPC concentration. This critical mass fraction of silicon oil corresponds to the solubility limit of the phospholipids in the organic phase mixture. Indeed, the mixture whitens for $\varphi > \varphi^*$, indicating a precipitation of the phospholipids. This observation implies that there is no direct way to form an adhesive emulsion for high bad solvent content. Third, this emulsion quenching always occurs at a bad solvent concentration for which a maximum contact angle of 90° is reached, independently of the phospholipid type.

It is nevertheless possible to form a stable bilayer while the concentration of bad solvent is beyond φ^*. Indeed, when the adhesive emulsion is formed using a PDMS microfluidic device, the chloroform can diffuse out, and the oil composition can thus be modified on-chip. Starting for $\varphi < \varphi^*$, the contact angle

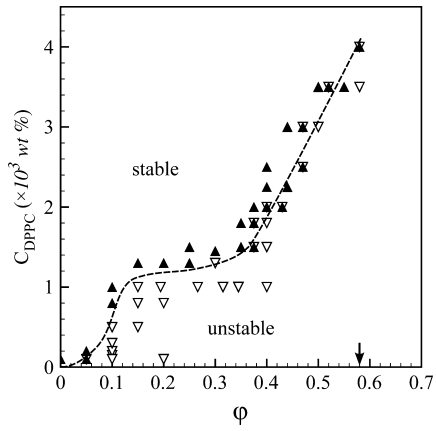

Figure 3. Stability diagram of a DPPC bilayer formed between two adhesive drops represented in the bad solvent mass fraction (φ)−phospholipids concentration (C_{DPPC}) plane. The dashed line delineates the frontier between the two states, i.e., (▲) stable and (▽) unstable. The critical mass fraction of silicone oil φ^* beyond which DPPC is no more soluble is equal to 0.58, as indicated by the arrow. Above that limit, instability precludes any observation of adhesion.

increases whenever the flow of the continuous phase is lowered or stopped. During the evaporation of the chloroform, which is illustrated by the first image row in Figure 4, the adhesion patch is expanding until the two droplets form a spherical object. The contact angle θ never exceeds 90° during the evaporation process, which is then the maximum reachable angle. The bilayer is then revealed by epifluorescence imaging when 1 wt % of NBD-lipids is added, as shown in the second image row in Figure 4. We also note that a further evaporation of chloroform leads to the formation of fluorescence spots on the surface of the drops that may indicate a coprecipitation of the phospholipids. Finally, as reported in the last image row in Figure 4, the two adhering drops having a lower contact angle are recovered when the chloroform is renewed by increasing or restarting the continuous phase flow. In addition, one may also note the diminution of droplet size that indicates a water escape during this experiment that lasts a few minutes. The composition of bad solvent in the oil phase went effectively over φ^*. Here, this strategy based on solvent evaporation is the only way to form stable bilayers approaching a zero surface

dx.doi.org/10.1021/la3003349 | Langmuir 2012, 28, 6291−6298

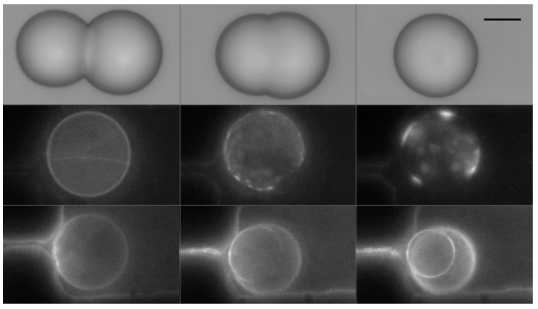

Figure 4. Time sequence showing an adhesive pair confined in a PDMS trap when chloroform is evaporated (first two rows) and then reintroduced (third row). The phenomenon is first observed in a bright field mode and then via epifluorescence microscopy by adding 1 wt % of NBD-PC. Time lapse goes from left to right with a time step of 1 min for the first two rows and 10 s for the third one. The scale bar is 50 μm.

tension such as vesicle membranes. Indeed, for $\theta = 90°$ and according to eq 1, the adhesion energy ΔF is equal to $2\gamma_0$, meaning that the surface tension γ_m of the monolayer composing the bilayer is $\gamma_m = \gamma_0 - \Delta F/2 = 0$.

What happens if the amount of surfactant is reduced? As reported in the stability diagram in Figure 3, for a given oil composition, there is a critical phospholipids concentration below which drops start to coalesce. In that condition, we observe that either the drops coalesce while the adhesive patch is being formed, or they fuse after the equilibrium angle has been reached. The times at which bilayers break down as a function of the bad solvent mass fraction φ and for a fixed amount of DPPC equal to 10^{-3} wt % are reported in Figure 5.

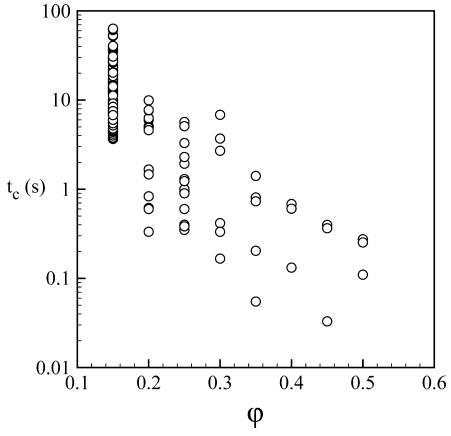

Figure 5. Distribution of the coalescence time t_c as a function of the amount of bad solvent φ for $C_{DPPC} = 10^{-3}$ wt %. We note that, at this surfactant concentration, the emulsion is stable for $\varphi \leq 0.1$ (Figure 3).

For φ larger than 0.35, the drops coalesce essentially before the adhesive patch attains its maximum size. For lower φ, the lifetime of the pairs starts to span from 0.2 to 10 s. More interestingly, for $\varphi = 0.15$, the lifetime of the adhering drop pair is also distributed, but it always lasts longer than the period of bilayer formation that is on the order of 1 s.

When two drops adhere, they create an additional surface since the volume is conserved. Therefore, phospholipids must diffuse fast enough to the surface in order to stabilize the adhering patch during its growth. Considering a bulk diffusion coefficient[27] $D = 8.10^{-10}$ m^2/s and a surface concentration $\Gamma^0 = 2.10^{-6}$ mol/m^2 of phospholipids in pure chloroform, an estimation of the characteristic bulk diffusion time is given by $(\Gamma^0/C_{DPPC})^2/D$. This characteristic time is about 10 s at $C_{DPPC} = 10^{-3}$ wt % and is larger than the characteristic time of a patch formation that is below 1 s for high concentrations of bad solvent. Moreover, we expect that the characteristic diffusion time should rise for mixtures of chloroform and silicone oil since the viscosity increases. Therefore, the competition between patch growth and transport of phospholipids presumably explains fast destabilization of adhering drop pairs that can occur for φ larger than 0.15 and always happen for φ larger than 0.35 (Figure 5).

The second regime of fusion takes place for a low amount of bad solvent. In that case, the bilayer has time to attain its maximum lateral size, but then its metastability nature manifests itself as it starts to rupture. As shown in Figure 6a, the

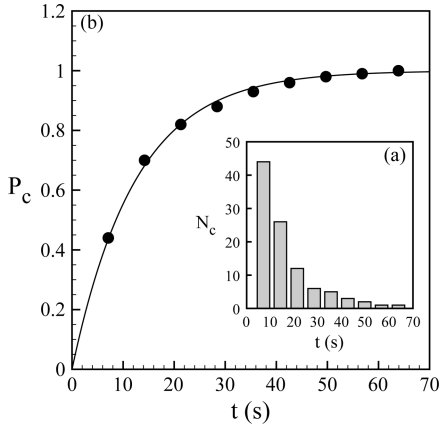

Figure 6. (a) Distribution N_c of the coalescence time of an adhering drop pair once the adhesion has been nucleated. (b) Probability P_c that an adhering drop pair coalesces at a time t, i.e., $P_c = \int_0^t N_c dt$. The continuous line represents an exponential function, which is a signature of a nucleation process. Experiments are done for $\varphi = 0.15$, $C_{DPPC} = 10^{-3}$ wt %, and with drops having a diameter of 250 μm.

distribution N_c of the coalescence time at $\varphi = 0.15$ is a decreasing function of time t. The corresponding probability to coalesce P_c after a period of time t, i.e., $P_c = \int_0^t N_c dt$, is reported in Figure 6b. This probability is close to the probability to observe a bilayer at a time t if the formation period, on the order of 1 s, is neglected. The evolution of P_c is well described by an exponential function, i.e., $P_c = 1 - \exp(-t/\tau_c)$, where τ_c, on the order of 13 s, can be assimilated to the mean lifetime of the bilayer. This exponential feature is reminiscent of a nucleation process that has been observed in foam bilayers[28] for low surfactant concentrations. The lifetime τ_c is linked to the activation energy barrier to overcome for nucleating an unstable pore into the membrane,[21] i.e., the pore expands and therefore leads to the rupture of the bilayer. Since the activation energy is intrinsically correlated to the surfactant layer properties,[21] the mean lifetime τ_c is expected to be a function of the phospholipids concentration as well as the mixture composition that tunes the bilayer state as discussed in the next section.

Adhesion Energy Landscape. We now establish the evolution of the adhesion energy as a function of the bad solvent for two phospholipids, DPPC and (Δ9-Cis)PC, at a concentration of 0.05 wt % and 0.1 wt %, respectively. These concentrations ensure the stability of the emulsions regardless

dx.doi.org/10.1021/la3003349 | Langmuir 2012, 28, 6291−6298

to the amount of silicone oil as long as it is beneath their precipitation limit. The difference between these two surfactants is the number of double links between carbon atoms on their tails: DPPC is saturated, while (Δ9-Cis)PC has two insaturations, one on each tail in a cis configuration. For each adhesive emulsion generated using these phospholipids, we measure the equilibrium contact angle for various compositions of bad solvent and deduce the adhesion energy ΔF from eq 1.

The evolution of the energy against the mass fraction φ of silicone oil is reported in Figure 7 for both phospholipids. The

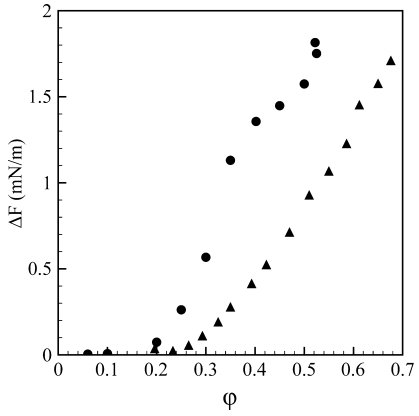

Figure 7. Evolution of the adhesion energy ΔF as a function of the mass fraction of silicone oil φ with an excess of phospholipds: (●) DPPC and (▲) (Δ9-Cis)PC.

adhesion energy increases with the amount of bad solvent as expected,[5] but one can notice two different behaviors. Even though the two curves display a region of lower rates of change in the range 0−0.3 of bad solvent, which we assimilate to a plateau, DPPC exhibits an additional plateau between 0.35 and 0.5. These plateaus correspond to a contact angle θ of 27° and 70°, respectively. One may also notice the difference between the precipitation limits φ^*: 0.58 for DPPC and 0.67 for (Δ9-Cis)PC. As previously noticed, these values correspond to the concentration of bad solvent for which the adhesive emulsion reaches a maximum contact angle of 90°. The surface tension γ_m of a monolayer forming a bilayer is determined by the mechanical equilibrium at the Plateau border (Figure 1b), namely from the Young−Dupré equation,[29] $\gamma_m = \gamma_0 \cos(\theta)$. The surface tension of the bilayer is then twice the surface tension of the monolayer.[30] Note in addition that, for $\theta = 90°$, the surface tension of the monolayers and the bilayer are null like for vesicle membranes. Using eq 1, the surface pressure $\Pi = \gamma_0 - \gamma_m$ acting on the monolayer is thus half the adhesion energy, i.e., $\Pi = \Delta F/2$. The surface pressure reflects the surface tension decrease from γ_0 to γ_m induced by adhesion and, as for the pressure acting on a Langmuir film, it describes the isotherm of adsorption of phospholipids from the oil reservoir toward the interfaces around adhering drops. Thus, the experimental plot of $\Delta F(\varphi)$ must also reflect the two-dimensional bilayer equation of state[31] $\Pi(\Gamma(\varphi))$, where Γ is the phospholipid surface concentration which is naturally controlled in our experiment by the solvent composition. By analogy, the piston of a Langmuir balance used to compress a monolayer is here reproduced by changing the amount of bad solvent. In other words, DPPC surface density within the adhesive monolayer is governed by its bulk chemical potential, which is directly linked to the solvent composition. We thus hypothesize that the plateaus of ΔF displayed in Figure 7 reflect the existence phase transitions undergone by adsorbed phospholipids. The first plateau that corresponds to an adhesion energy ΔF of the order of 0.1 mN/m should be a gas−liquid transition for the two kinds of phospholipids, while the second one occurring at $\Delta F \sim 1.5$ mN/m should be a liquid−gel transition for DPPC.[32] We note that at room temperature dense DPPC monolayers are in gel phase, whereas (Δ9-Cis)PC monolayers are in liquid phase.

To bring further evidence for these transitions, we make stoichiometric mixtures of the two phospholipids and follow the evolution of the adhesion energy as reported in Figure 8. The mass proportions of DPPC and (Δ9-Cis)PC that compose the mixture are 15/85, 50/50, 85/15, respectively. We observe a shift of the isotherm toward the one of the more abundant phospholipid as well as the presence of a second plateau revealing a liquid−gel transition. This is a well-known behavior for binary mixtures of miscible phospholipids. For instance, the transition temperatures in such mixtures are intermediate between the pure phospholipids transition temperatures and are closer to the more abundant one.[33] The present experimental strategy therefore offers a novel way to study the phase diagrams of bilayers, from a single phospholipid to a mixture of phospholipids, that are, as far as we know, difficult to obtain.

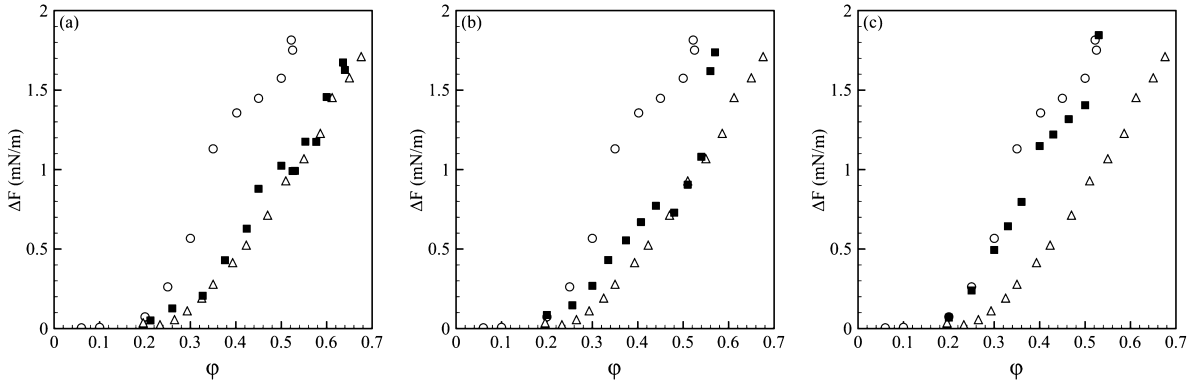

Figure 8. Evolution of the adhesion energy ΔF as a function of the oil composition φ for three phospholipid mixtures (■). The mass proportion of DPPC and (Δ9-Cis)PC are (a) 15/85, (b) 50/50, and (c) 85/15, respectively. The two adhesion energy curves for pure phospholipids are also reported: (○) DPPC and (Δ) (Δ9-Cis)PC.

dx.doi.org/10.1021/la3003349 | Langmuir 2012, 28, 6291−6298

Permeability to Water. We end this investigation by probing the semipermeability feature of the bilayer as a function of the solvent composition, and therefore as a function of the bilayer state. Here, only the flux of water through DPPC bilayers is studied. For that purpose, we set a chemical potential mismatch within an adhering drop pair. Experimentally, we produce two population of emulsion drops in a microfluidic device: one is made from pure water, and the other one is made from a solution containing 150 mM of $MgSO_4$. For convenience, the binary adhering drop pairs are stored in traps,[11] as shown in Figure 9. In order to distinguish the two

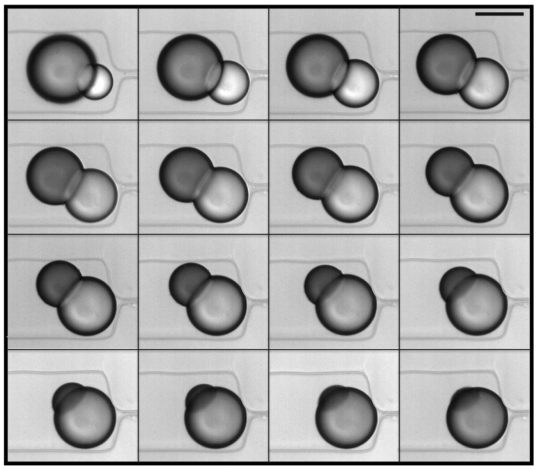

Figure 9. Time sequence showing the transport of water between two adhering drops having different compositions, pure water (labeled with methylene blue dye) and $MgSO_4$ solution at 150 mM. The time step between two frames is 3 s, and the scale bar is 50 μm.

populations of drops, methylene blue dye is added to the pure water drops. From the time sequence reported in Figure 9, we can observe a deflation of the pure water drop and a swelling of its neighbor that becomes slightly colored. We can conclude that water flows through the bilayer quicker than the methylene blue dye and of course much faster than the electrolytes, namely Mg^{2+} and SO_4^{2-}. During that period of time, the transport of water throughout the continuous phase and the PDMS matrix is negligible compared to the permeation time of water molecules through the membrane. We therefore assume mass conservation during that process. As previously demonstrated, the solubility-diffusion mechanism[34] accounts well for the water permeability of a lipid bilayers.[10,35] The hydrophobic membrane acts as a barrier for water molecules transport since the partition coefficient K is low and the diffusion coefficient D_m in the bilayer drops down. Indeed, according to this model, the permeability coefficient **P** of the bilayer is $\mathbf{P} = KD_m/\delta$, where δ is the membrane thickness. For dilute solutions, where the osmotic activity is proportional to the solute concentration, Fick's law leads to the following equation for the rate of change of the drop volume V:[35]

$$\frac{dV(t)}{dt} = -\mathbf{P}S(t)v_m\Delta C(t) \tag{2}$$

where v_m = 18 mL/mol is the water molar volume, S is the surface area of the bilayer, and $\Delta C(t)$ is the concentration difference of $MgSO_4$ between the two drops. We note that the permeability coefficient **P** is expressed in centimeters per second (cm/s). Since one drop does not contain any electrolytes, the concentration contrast of solutes is simply $\Delta C(t) = C_0 \times V_0/V(t)$, where V_0 is the initial drop volume and C_0 is the initial solute concentration set here to 150 mM. As observed in Figure 9, there exists a phase where the adhering patch size is almost constant. Within this period of time, when $S = C^{te}$, the time evolution of the swelling drop is obtained from the integration of eq 2

$$V(t)^2 = V_0^2\left(1 + 2\frac{\mathbf{P}Sv_mC_0}{V_0}t\right) \tag{3}$$

The permeability coefficient **P** can then be deduced from the measurement of $V(t)$. The height of the microfluidic channels used for trapping the drops is 67 μm. In order to keep the swelling drops spherical as long as possible, we form small salted drops with a diameter that spans from 22 to 40 μm. The volume of a swelled drop of radius R is given by $V = \pi h^2(3R - h)/3$, which corresponds to the volume of a truncated sphere where $h = R + (R^2 - R_p^2)^{1/2}$ and R_p is the radius of the patch. An example is reported in Figure 10 (a) where $(V(t)/V_0)^2$ is

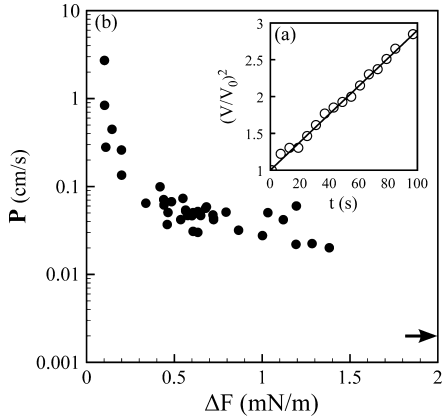

Figure 10. (a) Swelling kinetics of the salted drop from which the permeability coefficient **P** is deduced (eq 3). (b) Permeability coefficient to water of a DPPC bilayer as a function of the adhesion energy ΔF that tunes its fluidity. The arrow indicates the permeability of liposome membrane at room temperature that corresponds to θ = 90°.

plotted against t and exhibits a linear evolution. Using eq 3, **P** is deduced from the slope of $(V(t)/V_0)^2$. The permeability is then assessed for various solvent compositions. The permeability coefficient is reported in Figure 10b as a function of the adhesion energy ΔF. For a low quantity of bad solvent, and thus for a weak adhesion energy, the permeability strongly depends on ΔF. Indeed, P falls by more than 1 order of magnitude when ΔF is changed from 0.1 to 0.3 mN/m. Then, for ΔF larger than 0.5 mN/m, **P** is nearly constant until 1.5 mN/m. For a large amount of silicone oil, the experiments are difficult to carry on in PDMS devices since drops start to wet the wall. As previously discussed, the solvent composition tunes the packing state of the bilayer, namely, the surface area of the phospholipid molecules. The sharp decrease of **P** is correlated to the first phase transition, from gas to liquid, observed in the $[\varphi,\Delta F]$ plane and reported in Figure 7. This confirms previous observations on vesicle permeability to water that is correlated to the membrane fluidity.[36] More precisely, the lower the fluidity, the lower the permeability. What about the gel transition at ΔF = 1.5 mN/m? According to previous investigations,[37,38] the permeability of DPPC liposomes at

dx.doi.org/10.1021/la3003349 | Langmuir 2012, 28, 6291−6298

room temperature is about 4.10^{-3} cm/s. In our case, this situation corresponds to a contact angle between the adhering drops of 90°. The lowest permeability coefficient reported in Figure 10 is on the order of 2.10^{-2} cm/s. Therefore, another sharp decrease of **P** is expected for $\Delta F > 1.5$ mN/m in order to reach the liposome permeability. We conclude that the permeability must drop down when the DPPC bilayer is in the gel phase (Figure 7).

Furthermore, one can permeabilize bilayers to enable the transport of large molecules or electrolytes. A common way is to apply an electric field, which is known to induce the formation of transient pores into the membrane, is a phenomenon named electroporation.[39,40] In a recent publication,[11] we probed the response of adhesive emulsion bilayers under an electric field by using the same experimental strategy based on microfluidic technologies. We were able to map the behaviors of drop pairs within the adhesion energy-electric field intensity plane. We observe three distinct states: the pair can be either stable, though slightly deformed, or unzip and separate, or coalesce. We experimentally demonstrate that the force required to completely unzip a single bilayer matches the theoretical threshold predicted for the detachment of adhesive vesicles.[41,42] After unzipping, the drops repel each other under field. Then, they can attract each other when the electric field is turned off, meaning that each drop has now a net electrical charge. This is a demonstration of the occurrence of transient pores that allow charge transport across the membrane during the unzipping step. This charge exchange between the drops therefore leads to oppositely charged drops, which then naturally separate under field and attract one another in the absence of field. Besides, in the fluid and gel phases, we show that the transition between transient electroporation and coalescence is perfectly accounted for by the existence of an unique critical pore size above which the hole becomes unstable and expands. Therefore, when adhesion is increased, corresponding to a decrease of the membrane tension, coalescence will occur at a larger field such that the net surface energy gained by opening a constant hole size remains the same. This energy is assumed to be on the order of the thermal energy.[21] Finally, unzipping does not occur in the gas phase where the bilayer is poor in phospholipids. Indeed, the electric field easily leads to the appearance of unstable pores in the membrane that entail drop coalescence. This process probably occurs first, before drops are able to detach. Therefore, like for the permeability, the fluidity of the bilayer rules its behavior under an electric field.

CONCLUSION

This article reports a quantitative study on bilayer properties by using microfluidic technologies. The main novel aspect highlighted here is the way we are able to tune the surface tension of phospholipid bilayers formed between adhesive droplets and then to probe the consequences on their stability and permeability. Additionally, the present experimental strategy offers the possibility to investigate phase transitions occurring in bilayers, an investigation that is usually difficult to conduct. Indeed, the fluidity of the bilayer is here modified by simply changing the composition of the continuous phase that is an oil mixture. We also corroborate the fact that the permeability of the bilayer is linked to its fluidity. One open question to be addressed would be to determine the relationship between the continuous phase composition and the surface concentration of phospholipids. A natural follow-up is to investigate the properties of more complex bilayers by incorporating cholesterol and proteins to mimic cell membrane[7] as it has been recently demonstrated.[43,44]

AUTHOR INFORMATION

Corresponding Author

*E-mail: abdou-rachid.thiam@espci.fr.

Notes

The authors declare no competing financial interest.

ACKNOWLEDGMENTS

We are pleased to thank Enric Santanach, Jean-Daniel Emerard, and Jerome Delacotte for experimental set ups and surface tension measurements, and finally Jean Baudry, Bernard Cabane, and Philippe Poulin for fruitful discussions.

REFERENCES

(1) Israelachvili, J. N. *Intermolecular and Surface Forces*; Academic Press Inc.: New York, 1991.
(2) Leckband, D.; Israelachvili, J. Intermolecular forces in biology. *Q. Rev. Biophys.* **2001**, *34*, 105−267.
(3) Leal-Calderon, F.; Schmitt, V.; Bibette, J. *Emulsion Science - Basic Principles*; Springer: New York, 2007.
(4) Lipowsky, R. The conformation of membranes. *Nature* **1991**, *349*, 475−481.
(5) Poulin, P.; Bibette, J. Adhesion of water droplets in organic solvent. *Langmuir* **1998**, *14*, 6341−6343.
(6) Funakoshi, K.; Suzuki, H.; Takeuchi, S. Lipid bilayer formation by contacting monolayers in a microfluidic device for membrane protein analysis. *Anal. Chem.* **2006**, *78*, 8169−8174.
(7) Lipowsky, R., Sackmann, E., Eds. *Structure and Dynamics of Membranes, Handbook of Biological Physics*; Elsevier: New York, 1995; Vol. *1*.
(8) Sackmann, E. Supported membranes: Scientific and practical applications. *Science* **1996**, *271*, 43−48.
(9) Neumann, E.; Sowers, E. A.; Jordan, C. A. *Electroporation and Electrofusion in Cell Biology*; Plenum Press, New York, 1989.
(10) Paula, S.; Volkov, A. G.; VanHoek, A. N.; Haines, T. H.; Deamer, D. W. Permeation of protons, potassium ions, and small polar molecules through phospholipid bilayers as a function of membrane thickness. *Biophys. J.* **1996**, *70*, 339−348.
(11) Thiam, A. R.; Bremond, N.; Bibette, J. Adhesive emulsion bilayers under an electric field: From unzipping to fusion. *Phys. Rev. Lett.* **2011**, *107*, 068301.
(12) Aronson, M. P.; Princen, H. M. Contact angles associated with thin liquid-films in emulsions. *Nature* **1980**, *286*, 370−372.
(13) Dixit, S. S.; Kim, H.; Vasilyev, A.; Eid, A.; Faris, G. W. Light-driven formation and rupture of droplet bilayers. *Langmuir* **2010**, *26*, 6193−6200.
(14) Yeung, A.; Dabros, T.; Masliyah, J.; Czarnecki, J. Micropipette: A new technique in emulsion research. *Colloids Surf., A* **2000**, *174*, 169−181.
(15) Jorgensen, L.; Kim, D. H.; Vermehren, C.; Bjerregaard, S.; Frokjaer, S. Micropipette manipulation: A technique to evaluate the stability of water-in-oil emulsions containing proteins. *J. Pharm. Sci.* **2004**, *93*, 2994−3003.
(16) Bremond, N.; Thiam, A. R.; Bibette, J. Decompressing emulsion droplets favors coalescence. *Phys. Rev. Lett.* **2008**, *100*, 024501.
(17) Thiam, A. R.; Bremond, N.; Bibette, J. Breaking of an emulsion under an ac electric field. *Phys. Rev. Lett.* **2009**, *102*, 188304.
(18) Baret, J. C.; Kleinschmidt, F.; El Harrak, A.; Griffiths, A. D. Kinetic aspects of emulsion stabilization by surfactants: A microfluidic analysis. *Langmuir* **2009**, *25*, 6088−6093.
(19) Bremond, N.; Domejean, H.; Bibette, J. Propagation of drop coalescence in a two-dimensional emulsion: A route towards phase inversion. *Phys. Rev. Lett.* **2011**, *106*, 214502.

(20) Anna, S. L.; Bontoux, N.; Stone, H. A. Formation of dispersions using "flow focusing" in microchannels. *Appl. Phys. Lett.* **2003**, *82*, 364−366.
(21) Kabalnov, A.; Wennerstrom, H. Macroemulsion stability: The oriented wedge theory revisited. *Langmuir* **1996**, *12*, 276−292.
(22) Utada, A. S.; Lorenceau, E.; Link, D. R.; Kaplan, P. D.; Stone, H. A.; Weitz, D. A. Monodisperse double emulsions generated from a microcapillary device. *Science* **2005**, *308*, 537−541.
(23) Evans, E.; Needham, D. Physical-properties of surfactant bilayer-membranes - Thermal transitions, elasticity, rigidity, cohesion, and colloidal interactions. *J. Phys. Chem.* **1987**, *91*, 4219−4228.
(24) Leal, L. G. Flow induced coalescence of drops in a viscous fluid. *Phys. Fluids* **2004**, *16*, 1833−1851.
(25) Lai, A.; Bremond, N.; Stone, H. A. Separation-driven coalescence of droplets: An analytical criterion for the approach to contact. *J. Fluid Mech.* **2009**, *632*, 97−107.
(26) Chan, D. Y. C.; Klaseboer, E.; Manica, R. Dynamic deformations and forces in soft matter. *Soft Matter* **2009**, *5*, 2858−2861.
(27) Li, J. B.; Fainerman, V. B.; Miller, R. Adsorption kinetics of phospholipids at the chloroform/water interface studied by drop volume and pendant drop techniques. *Langmuir* **1996**, *12*, 5138−5142.
(28) Exerowa, D.; Kashchiev, D.; Platikanov, D. Stability and permeability of amphiphile bilayers. *Adv. Colloid Interface Sci.* **1992**, *40*, 201−256.
(29) de Gennes, P.; Brochard-Wyart, F.; Quéré, D. *Gouttes, Bulles, Perles et Ondes*; Belin: Paris, 2002.
(30) Toshev, B. V. Thermodynamic theory of thin liquid films including line tension effects. *Curr. Opin. Colloid Interface Sci.* **2008**, *13*, 100−106.
(31) MacDonald, R. C.; Simon, S. A. Lipid monolayer states and their relationships to bilayers. *Proc. Natl. Acad. Sci. U.S.A.* **1987**, *84*, 4089−4093.
(32) Kaganer, V. M.; Möhwald, H.; Dutta, P. Structure and phase transitions in Langmuir monolayers. *Rev. Mod. Phys.* **1999**, *71*, 779−819.
(33) Garidel, P.; Blume, A. Miscibility of phospholipids with identical headgroups and acyl chain lengths differing by two methylene units: Effects of headgroup structure and headgroup charge. *Biochim. Biophys. Acta, Biomembr.* **1998**, *1371*, 83−95.
(34) Zwolinski, B. J.; Eyring, H.; Reese, C. E. Diffusion and membrane permeability. *J. Phys. Colloid Chem.* **1949**, *53*, 1426−1453.
(35) Olbrich, K.; Rawicz, W.; Needham, D.; Evans, E. Water permeability and mechanical strength of polyunsaturated lipid bilayers. *Biophys. J.* **2000**, *79*, 321−327.
(36) Lande, M. B.; Donovan, J. M.; Zeidel, M. L. The relationship between membrane fluidity and permeabilities to water, solutes, ammonia, and protons. *J. Gen. Physiol.* **1995**, *106*, 67−84.
(37) Graziani, Y.; Livne, A. Water permeability of bilayer lipid membranes: Sterol-lipid interaction. *J. Membr. Biol.* **1972**, *7*, 275−284.
(38) Marrink, S.-J.; Berendsen, H. J. C. Simulation of water transport through a lipid membrane. *J. Phys. Chem.* **1994**, *98*, 4155−4168.
(39) Weaver, J. C.; Chizmadzhev, Y. Theory of electroporation: A review. *Bioelectroch. Bioenerg.* **1996**, *41*, 135−160.
(40) Dimova, R.; Bezlyepkina, N.; Jordo, M. D.; Knorr, R. L.; Riske, K. A.; Staykova, M.; Vlahovska, P. M.; Yamamoto, T.; Yang, P.; Lipowsky, R. Vesicles in electric fields: Some novel aspects of membrane behavior. *Soft Matter* **2009**, *5*, 3201−3212.
(41) Brochard-Wyart, F.; de Gennes, P. G. Unbinding of adhesive vesicles. *C. R. Phys.* **2003**, *4*, 281−287.
(42) Pierrat, S.; Brochard-Wyart, F.; Nassoy, P. Enforced detachment of red blood cells adhering to surfaces: Statics and dynamics. *Biophys. J.* **2004**, *87*, 2855−2869.
(43) Thutupalli, S.; Herminghaus, S.; Seemann, R. Bilayer membranes in micro-fluidics: From gel emulsions to soft functional devices. *Soft Matter* **2011**, *7*, 1312−1320.
(44) Villar, G.; Heron, A. J.; Bayley, H. Formation of droplet networks that function in aqueous environments. *Nat. Nano* **2011**, *6*, 803−808.